


**Ballistic thermal rectification in asymmetric homojunctions**

Yuanchen Wu<sup>✉,\*</sup>, Yu Yang<sup>✉,\*</sup>, Longkai Lu<sup>✉</sup>, Tingting Wang, Lei Xu, Zhizhou Yu<sup>✉,†</sup> and Lifa Zhang<sup>‡</sup>  
*NNU-SULI Thermal Energy Research Center (NSTER) and Center for Quantum Transport and Thermal Energy Science (CQTES),  
 School of Physics and Technology, Nanjing Normal University, Nanjing 210023, China*

 (Received 7 March 2021; accepted 10 May 2021; published 25 May 2021)

Ballistic thermal rectification is of significance for the management of thermal transport at the nanoscale since the size of thermal devices shrinks down to the phonon mean free path. By using the single-particle Lorentz gas model, the ballistic thermal transport in asymmetric homojunctions is investigated. The ballistic thermal rectification of the asymmetric rectangular homojunction is enhanced by the increasing structural asymmetry. A hyperbolic tangent profile is introduced to the interface to study the effect of interface steepness on thermal transport. We find that the thermal rectification ratio increases with the decreasing interface steepness, indicating that a gradual interface is of benefit to increase the thermal rectification. Moreover, the thermal rectification of the asymmetric homojunction can be improved by either increasing the temperature gradient or decreasing the average temperature of two heat sources.

DOI: [10.1103/PhysRevE.103.052135](https://doi.org/10.1103/PhysRevE.103.052135)

**I. INTRODUCTION**

With the size of integrated circuit chip shrinks in recent decades, thermal management is attracting increasing attention due to the increasing power density that brings a great challenge in energy conversion and dissipation. Similar to electronic devices, many functional thermal devices are proposed to manipulate the heat flow, such as thermal diodes [1–10], thermal transistors [11–17], thermal memories [18–20] and thermal logic circuits [21–23]. The thermal diode is a very basic component of thermal devices in which the forward and backward heat flows are asymmetric when the direction of the temperature gradient is reversed. The necessary conditions to achieve thermal rectification are the intrinsic asymmetry and nonlinearity in thermal devices. Since the prototypical thermal diode was proposed theoretically in 2004 [3], the thermal rectification effect has been extensively studied in inherent anharmonic systems with structural asymmetry [4–10].

Recently, with the rapid development in nanotechnology, ballistic thermal transport is dominated in nanodevices since the size of thermal devices can be compared with the phonon mean free path [2]. For instance, excellent thermal rectification was obtained in asymmetric graphene nanoribbons by using molecular dynamics simulations [24]. It is quite crucial to understand the ballistic thermal transport in harmonic systems. Zhang *et al.* investigated the ballistic thermal rectification in three-terminal asymmetric nanojunctions using the nonequilibrium Green's function method [25]. It was found that apart from asymmetry, the phonon incoherence instead of the nonlinearity is the necessary condition for thermal

rectification, which can be induced by the scattering control terminal. However, whether the ballistic thermal rectification can be achieved in a two-terminal ballistic system is still unknown. It is the purpose of this paper to address this important issue.

The Lorentz gas model, which was first proposed to investigate the motion of electrons in metallic bodies [26,27], has been widely used to study the thermal transport in quasi-one-dimensional systems such as heat conduction of layered structures [28,29], boundary effect on thermal transport [30], thermal Hall effect [31], and random walk theory [32]. These studies show that the Lorentz gas model is a simple and efficient tool to study thermal transport. In this paper, the single-particle Lorentz gas model is employed to study the thermal transport in asymmetric homojunctions. There is no scattering in the single-particle Lorentz gas model except the interface region. The corresponding thermal transport can thus be considered to be ballistic. The effect of structural asymmetry and interface steepness on the ballistic thermal rectification is investigated. For the asymmetric rectangular homojunction, the stronger structural asymmetry, namely, the larger width ratio of two heat sources results in the larger thermal rectification. For the asymmetric homojunction with a hyperbolic tangent interface, a weaker thermal rectification is found for the system with a larger interface steepness. In addition, the thermal rectification increases with the increasing temperature gradient and the increasing average temperature of two heat sources.

The remainder of this paper is organized as follows. In Sec. II, the ballistic thermal transport in asymmetric rectangular homojunctions is studied and the effect of structural asymmetry on the thermal rectification is discussed. In Sec. III, a hyperbolic tangent profile is introduced to the interface and the thermal rectification of asymmetric homojunctions with different interface steepness is studied. Finally, a brief conclusion is given in Sec. IV.

\*These two authors contributed equally to this work.

<sup>†</sup>yuzhizhou@njnu.edu.cn

<sup>‡</sup>phyzlf@njnu.edu.cn

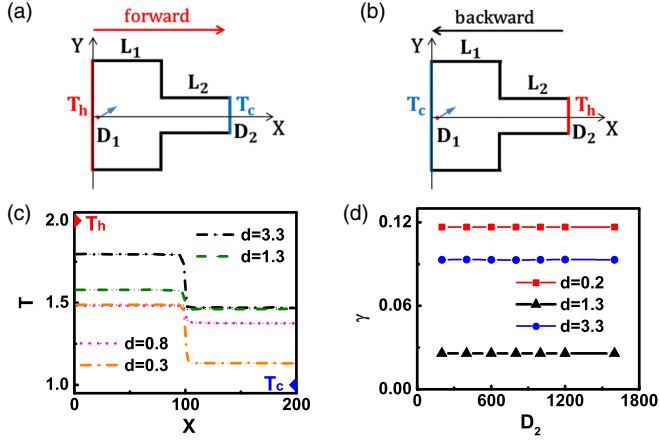


FIG. 1. Schematic diagram of the asymmetric rectangular homojunction in (a) forward direction and (b) backward direction. The asymmetric homojunction is composed of two rectangles having length  $L_1$  and  $L_2$ , and width  $D_1$  and  $D_2$ . The temperatures of heat reservoirs on the hot side and cold side are denoted by  $T_h$  and  $T_c$ , respectively. (c) Temperature distribution along the transport direction with different width ratio for the asymmetric rectangular homojunction with  $D_2=200$ ,  $L_1 = L_2 = 100$ ,  $T_h=2.0$ , and  $T_c=1.0$  in the forward direction. (d) Thermal rectification ratio is independent with the width of asymmetric rectangular homojunction under a given width ratio.

## II. THERMAL TRANSPORT IN ASYMMETRIC RECTANGULAR HOMOJUNCTIONS

The schematic setup of asymmetric homojunctions for the Lorentz gas model is composed of two rectangles, as shown in Figs. 1(a) and 1(b). The lengths of the two rectangles are  $L_1$  and  $L_2$ , and their widths are  $D_1$  and  $D_2$ . In previous studies, it was found that the thermal conductivity is independent of the length of the Lorentz gas model. The thermal rectification is also independent of the length and width of the Lorentz gas model with a fixed width ratio of two heat reservoirs [10,30,33]. In order to study the effect of asymmetry in width on the thermal rectification in ballistic systems, the width ratio is defined as  $d = \frac{D_1}{D_2}$ . The temperatures of heat reservoirs on the hot side and cold side are denoted by  $T_h$  and  $T_c$ , respectively. Although previous studies on thermodynamics in the Katz-Lebowitz-Spohn lattice gas model show that both the chemical potential and temperature need to be defined for the driven system [34], only the temperature is enough to describe the heat reservoirs in our single-particle Lorentz gas model since we focus on thermal transport in a homogeneous junction without multiphase coexistence. At a certain moment, a particle is emitted from the heat reservoir at a random position and the velocity of the particle follows the Maxwell velocity distribution [31,33],

$$P(v_{\parallel}) = \frac{|v_{\parallel}|}{T} e^{-v_{\parallel}^2/(2T)}, \quad (1)$$

$$P(v_{\perp}) = \frac{1}{\sqrt{2\pi T}} e^{-v_{\perp}^2/(2T)}. \quad (2)$$

Here,  $v_{\parallel}$  and  $v_{\perp}$  represent the  $x$ - and  $y$ -axis component of the velocity, respectively.  $T$  is the temperature of the heat

reservoir. The particle mass ( $m$ ) and the Boltzmann constant ( $k_B$ ) are set to 1 for simplicity. The collisions with boundaries are described as purely elastic collisions. When the particle comes to the heat reservoir, it is absorbed and another particle is emitted from the heat reservoir at a random position in return.

When the system reaches a stationary state after a long enough time, the temperature distribution, heat flow, and thermal conductivity of the system can be obtained. In our simulation, the space of our model is divided into many small regions along the transport direction and the average kinetic energy in each region is considered to be proportional to its temperature due to the equipartition theorem. Therefore, the temperature distribution along the transport direction can be given by

$$T_m = \frac{2}{3} E_m. \quad (3)$$

Here,  $T_m$  and  $E_m$  represent the temperature and average kinetic energy of the  $m$ th region, respectively.

In Fig. 1(c), we plot the temperature distribution along the transport direction with different width ratio for the asymmetric rectangular homojunction in the forward direction. The temperature shows the same value in the whole narrow or wide region, and a sudden change occurs at the interface, which indicates the ballistic behavior of particle transport in the narrow and wide region. Moreover, the single-particle Lorentz model does not obey Fourier's heat conduction law in the ballistic regime. The temperature at the narrow region is the same as the average temperature of two heat sources, while the temperature at the wide region decreases with the decreasing width ratio  $d$ .

The forward (backward) heat flow  $J_{f(b)}$  can be obtained from the net energy change of heat source and the total time,

$$J_{f(b)} = \frac{\Delta E}{t_{f(b)}}, \quad (4)$$

$$\Delta E = |E^{\text{absorbed}} - E^{\text{released}}|. \quad (5)$$

Since the energy released by the hot source equals that absorbed by the cold source, we only need to calculate the net change of energy for absorbing and releasing the particle at one heat source. When the temperature gradient applied on two heat reservoirs is reversed, the temperature distribution in the forward and backward case is strongly different. Therefore, the forward and backward heat flows across the asymmetric homojunction are different, which results in the thermal rectification effect. The thermal rectification ratio  $\gamma$  is defined as [10,31],

$$\gamma = \left| \frac{J_f - J_b}{J_f + J_b} \right|. \quad (6)$$

Note that both the forward and backward heat flows are restricted to be positive here. It is easy to see that there is no thermal rectification effect ( $\gamma = 0$ ) if the heat flows in the forward and backward directions are symmetrical ( $J_f = J_b$ ) and the thermal rectification ratio reaches the maximum ( $\gamma = 1$ ) if the heat flow in either direction disappears.

Figure 1(d) presents the thermal rectification ratio  $\gamma$  as a function of  $D_2$  under a certain width ratio  $d$ . It is found that the thermal rectification ratio only depends on the width

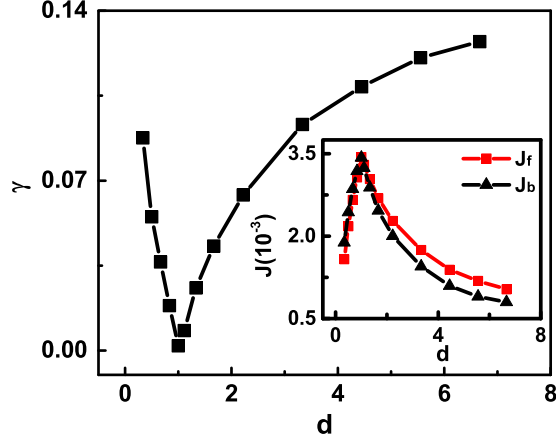


FIG. 2. Thermal rectification ratio as a function of the width ratio. Inset: The corresponding forward and backward heat flows as a function of the width ratio.

ratio and is independent of the widths of the asymmetric rectangular homojunction when the width ratio is fixed. The thermal rectification ratio as a function of the width ratio is then plotted in Fig. 2. For the symmetrical homojunction ( $d = 1$ ), the thermal rectification ratio is zero, namely, there is no thermal rectification effect. For asymmetrical rectangular homojunctions, the thermal rectification ratio increases with the increasing asymmetry of the system, which is because the difference between the forward and backward heat flows increases with the increasing width ratio, as shown in the inset of Fig. 2. This can be further explained by the elapsed time difference between the forward and backward directions. From Eq. (A6), it can be found that  $t_f - t_b$  is determined by the transmission probability through the interface, which is inversely proportional to the width ratio  $d$ . Therefore,  $t_f$  becomes much smaller than  $t_b$  as the structural asymmetry increases, which results in the enlarged difference between forward and backward heat flows. Moreover, when the width ratio changes from  $d < 1$  to  $d > 1$ , the forward heat flow changes from smaller to larger than the backward heat flow, resulting in the reversion of thermal rectification when wider heat source changes from hot to cold.

From the difference between forward and backward heat flows, it can be found that in asymmetric two-terminal systems, the ballistic thermal rectification is obtained because of the incoherent phonon scattering at the interface. Therefore, apart from the structural asymmetry, phonon incoherence induced by the scattering interface is the necessary condition to achieve ballistic thermal rectification in two-terminal systems. Our result agrees with previous studies on the necessary conditions for ballistic thermal rectification in three-terminal systems, namely, asymmetry and phonon incoherence [25].

### III. THERMAL TRANSPORT IN ASYMMETRIC HOMOJUNCTIONS WITH A HYPERBOLIC TANGENT INTERFACE

In order to study the effect of interface configuration on the thermal rectification, a hyperbolic tangent interface with a length of  $L_3$  is introduced between two rectangles of the asymmetric homojunction, as shown in Fig. 3(a). The total

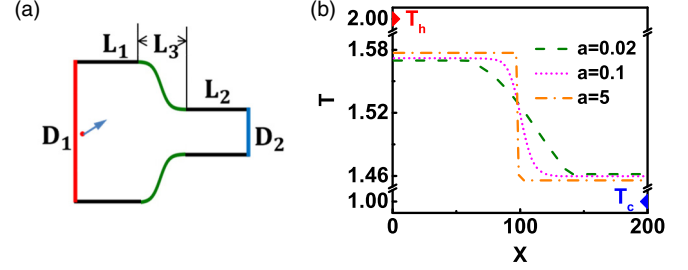


FIG. 3. (a) Schematic diagram of the asymmetric homojunction with a hyperbolic tangent interface. (b) Temperature distribution along the transport direction of asymmetric homojunctions with different steepness of the interface. The parameters of the model is set to be  $D_1 = 200$ ,  $D_2 = 150$ ,  $L_1 = L_2 = 60$ ,  $L_3 = 80$ ,  $T_h = 2.0$ , and  $T_c = 1.0$ .

length of the model is kept as the same as that without the transition region. The profile of the hyperbolic tangent interface is described by

$$y = A \tanh(ax). \quad (7)$$

Here,  $a$  is a non-negative real number used to describe the steepness of the interface.  $A = \frac{1}{4}(D_2 - D_1) \coth(\frac{1}{2}aL_3)$  is determined by the width difference between two heat sources and the length of interface. For a large  $a$ , the asymmetric homojunction becomes a rectangular homojunction as discussed in the previous section. For the system with a tiny  $a$  close to 0, a trapezoidal interface is introduced to the asymmetric homojunction. The temperature distributions of systems with different sharpness of the interface along the transport direction are presented in Fig. 3(b). When the interface is no longer vertical, a temperature gradient can be found in the hyperbolic tangent interface region.

Figure 4(a) presents the thermal rectification of the asymmetric homojunction as a function of interface steepness under different thermal gradients. The average source temperature, namely,  $T = (T_h + T_c)/2$  is fixed. When the interface steepness increases, the thermal rectification ratio first decreases rapidly and then gradually approaches that of the asymmetric homojunction without interfacial transition layer. Such a trend of thermal rectification does not change for systems with a fixed average source temperature under different thermal gradients. Moreover, the thermal rectification ratio of the asymmetric homojunction with  $a = 0.02$  is about 1.8 times that of the system with  $a = 5$  under different thermal gradients, indicating that the thermal rectification ratio can be greatly enhanced by a gradual interface. Our results agree with previous molecular dynamics simulations on the thermal rectification in asymmetric graphene nanoribbons in which the rectification ratio of the trapezia-shaped graphene junction is higher than that of the rectangular graphene junction [24].

The forward and backward heat flows for systems with different interface steepness are calculated to understand the thermal rectification, as shown in the inset of Fig. 4(a). It is found that the forward heat flow of the asymmetric homojunction is always greater than the backward one. The forward and backward heat flows gradually approach each other with the increasing interface steepness. The behavior of heat flows can be explained by the total time  $t_{f(b)}$  of particle transport (see

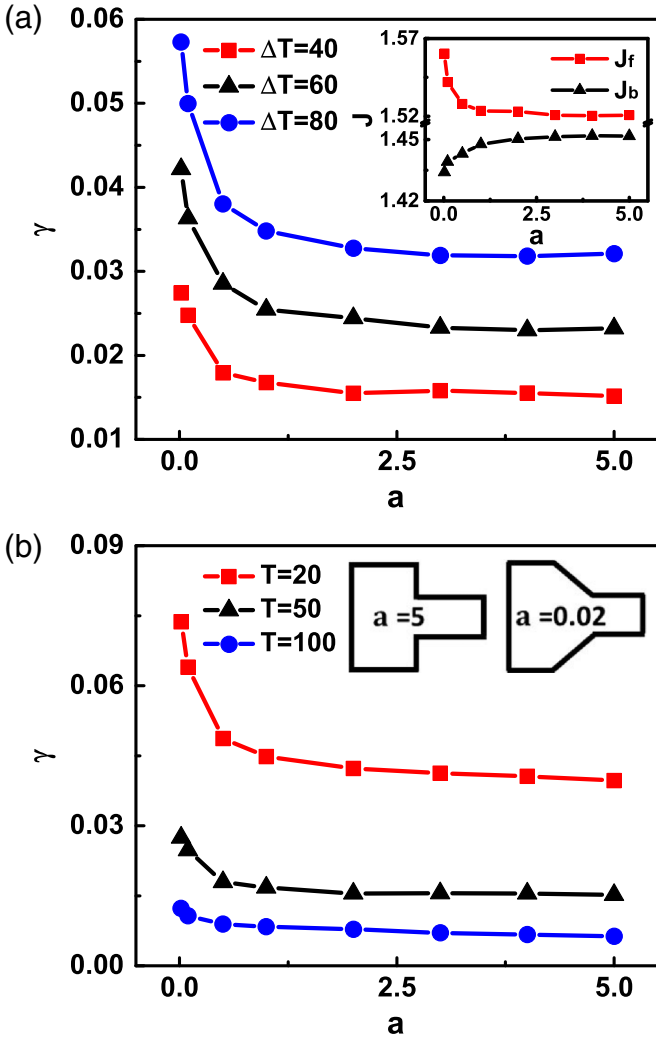


FIG. 4. (a) Thermal rectification ratio of asymmetric homojunctions as a function of interfacial steepness under different temperature gradients. The temperatures of the hot and cold sources are set to be  $T_h = T + \Delta T/2$  and  $T_c = T - \Delta T/2$ , respectively and the average source temperature is set to be  $T = 100$ . Inset: the corresponding forward and backward heat flows for the case of  $\Delta T = 60$ . (b) thermal rectification ratio of asymmetric homojunctions as a function of interfacial steepness under different average source temperatures. The temperature difference is set to be  $\Delta T = 20$ . Inset: schematic diagrams of asymmetric homojunction models with  $a = 5$  and  $a = 0.02$ .

details in the Appendix). For systems with a sharp interface, particles are strongly scattered at the interface, resulting in almost the same forward and backward heat flows and further a weak thermal rectification effect. While for systems with a relatively smooth interface, the forward heat flow becomes much larger than the backward one, which leads to a large thermal rectification ratio. Moreover, similar behavior of the thermal rectification can be found for asymmetric homojunctions with a fixed temperature difference under different average source temperatures, as shown in Fig. 4(b).

In order to study the relations between the thermal rectification and the temperatures of heat sources, we also calculated the thermal rectification ratio of asymmetric homojunctions

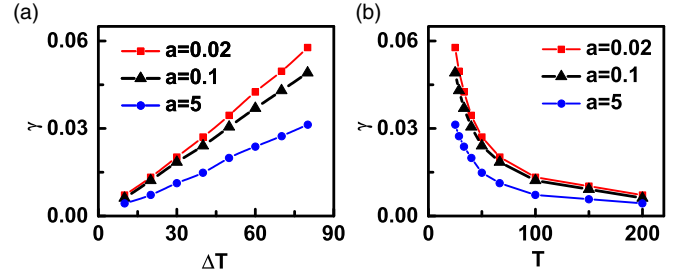


FIG. 5. (a) Thermal rectification ratio of asymmetric homojunctions as a function of temperature difference between two heat sources under different interfacial steepness. The average source temperature is set to be  $T = 100$ . (b) Thermal rectification ratio of asymmetric homojunctions as a function of average source temperature under different interfacial steepness. The temperature difference is set to be  $\Delta T = 20$ .

with a fixed average source temperature under different temperature gradients, as shown in Fig. 5(a). It is found that the thermal rectification ratio increases linearly with the increasing temperature difference between two heat sources. This is because the particle released by the heat source with a higher temperature is easier to reach the narrow region, which results in a larger forward heat flow, and vice versa. The increase of the forward heat flow and the decrease of the backward heat flow give rise to the improvement of thermal rectification for systems with increasing temperature differences between two heat sources. Moreover, the slope of the thermal rectification ratio decreases with the rise of interfacial steepness. Figure 5(b) presents the thermal rectification ratio of asymmetric homojunctions with a fixed temperature gradient under different average source temperatures. The thermal rectification ratio decreases monotonously when the temperatures of heat sources increase simultaneously due to the increasing forward and backward heat flows.

#### IV. CONCLUSION

In summary, we have studied the ballistic thermal rectification in asymmetric homojunctions using the single-particle Lorentz gas model. The asymmetric rectangular homojunction is first considered and its thermal rectification increases with the increasing structural asymmetry, namely, the width ratio of two heat sources. The phonon incoherence induced by the scattering interface and the structural symmetry are two necessary conditions for ballistic thermal rectification in two-terminal systems, which is similar to the necessary conditions for thermal rectification in previous studies.

To further study the effect of interface geometry on thermal transport, a hyperbolic tangent profile is introduced to the interface of asymmetric homojunctions. It is found that the thermal rectification ratio increases with the decreasing interfacial steepness, which shows the thermal rectification can be significantly enhanced by a gradual interface. We also investigated the temperature dependence of the thermal rectification in asymmetric homojunctions with a hyperbolic tangent interface. The thermal rectification can be improved by either increasing the temperature gradient or decreasing the average temperature of two heat sources. Our numerical



simulation on ballistic thermal rectification in two-terminal systems may provide potential guidance for the design of thermal diodes based on the quasi-one-dimensional materials within the ballistic transport regime.

### ACKNOWLEDGMENTS

This work was financially supported by the National Natural Science Foundation of China (Grants No. 12074190, No. 11975125, No. 11890703, and No. 11874221). Y.Y. acknowledges the Postgraduate Research & Practice Innovation Program of Jiangsu Province (Grant No. KYCX20\_1229).

### APPENDIX: FORWARD AND BACKWARD HEAT FLOWS IN ASYMMETRIC HOMOJUNCTIONS

We first consider the forward and backward heat flows in asymmetric rectangular homojunctions. When the number of transports  $N$  is large enough, the system can be considered to be thermal nonequilibrium stationary states and the average energy of one single transport ( $\overline{\Delta E}$ ) can be expressed as

$$\overline{\Delta E} = \frac{\Delta E}{N} = \frac{\bar{v}_h^2 - \bar{v}_c^2}{2}. \quad (\text{A1})$$

Here,  $\bar{v}_{h(c)}$  represents the average velocity (root mean square velocity) of particle emitted from the heat source with temperature  $T_{h(c)}$ . Since the average energy of one single transport is the same for the cases in the forward and backward direction, the forward and backward heat flows are only determined by the total time  $t_{f(b)}$  of particle transport according to Eq. (4). We can write the total time  $t_{f(b)}$  as

$$t_{f(b)} = N[t_{f(b),LL} + t_{f(b),LR} + t_{f(b),RL}]. \quad (\text{A2})$$

Here,  $t_{f(b),\alpha\beta}$  is the time for one transport of the particle in the forward (backward) direction from its emission from the  $\alpha$  heat source to its absorption by the  $\beta$  heat source, which can be expressed as

$$t_{f(b),LL} = (1 - \xi) \frac{2L_1}{\bar{v}_{h(c)}}, \quad (\text{A3})$$

$$t_{f(b),LR} = \xi \frac{L_1 + L_2}{\bar{v}_{h(c)}}, \quad (\text{A4})$$

$$t_{f(b),RL} = \xi \frac{L_1 + L_2}{\bar{v}_{c(h)}}. \quad (\text{A5})$$

Here,  $\xi$  refers to the transmission probability through the interface. Since  $\bar{v}_h > \bar{v}_c$ , we can easily obtain,

$$t_f - t_b = 2(1 - \xi)L_1 \left( \frac{1}{\bar{v}_h} - \frac{1}{\bar{v}_c} \right) < 0. \quad (\text{A6})$$

Therefore, the forward heat flow  $J_f$  of the asymmetric rectangular homojunction should be greater than the backward one  $J_b$ .

We then consider the asymmetric homojunction with a hyperbolic tangent interface and compare the heat flows for systems with different interface steepness. In the forward direction, the difference of total time for particle transport between two systems with different interface steepness  $a$  can be given by

$$\delta t_f = N(\eta_{LL}\delta t_{f,LL} + \eta_{LR}\delta t_{f,LR} + \eta_{RL}\delta t_{f,RL}). \quad (\text{A7})$$

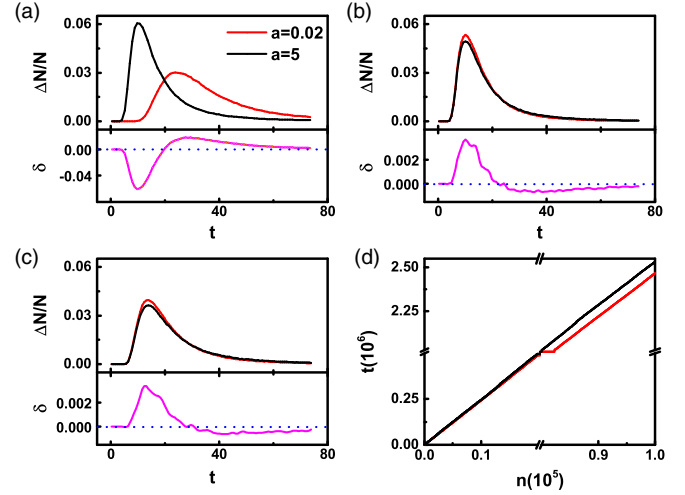


FIG. 6. (a) Upper panel: the probability distribution function of  $t_{f,LL}$  for a particle emitted from the left heat source and finally absorbed by the left heat source in the forward direction for the case of  $a = 0.02$  (red line) and  $a = 5$  (black line). Lower panel: the difference of the probability distribution function of  $t_{f,LL}$  between the case of  $a = 0.02$  and  $a = 5$ . (b) Probability distribution function of  $t_{f,LR}$  for the case of  $a = 0.02$  (red line) and  $a = 5$  (black line) and their difference. (c) Probability distribution function of  $t_{f,RL}$  for the case of  $a = 0.02$  (red line) and  $a = 5$  (black line) and their difference. (d) Cumulative distribution function of the total transports for the case of  $a = 0.02$  (red line) and  $a = 5$  (black line).

Here,  $\delta t_{f,\alpha\beta}$  is the difference of  $t_{f,\alpha\beta}$  between two systems with different interface steepness  $a$ .  $\eta_{\alpha\beta} = N_{\alpha\beta}/N$  with  $N_{\alpha\beta}$  the number of transports for the particle emitted from the  $\alpha$  heat source and absorbed by the  $\beta$  heat source. From the probability distribution function of  $t_{f,\alpha\beta}$  shown in Fig. 6, it is found that when the interface steepness increases, the elapsed time of a particle released and adsorbed by the same heat source becomes longer ( $\delta t_{f,LL} > 0$ ), while the elapsed time for a particle emitted from one heat source and adsorbed by another heat source becomes shorter ( $\delta t_{f,LR} < 0$  and  $\delta t_{f,RL} < 0$ ). In our simulation, one can find the following details when the interface steepness changes from  $a = 0.02$  to  $a = 5$ :

$$\begin{aligned} \eta_{LL} &= 0.146, & \eta_{LR} &= \eta_{RL} = 0.427, \\ \delta t_{f,LL} &= 1.873, & \delta t_{f,LR} &= -0.308, & \delta t_{f,RL} &= -0.465. \end{aligned} \quad (\text{A8})$$

Since the number of transports  $N_{LR}$  and  $N_{RL}$  is much larger than  $N_{LL}$ , the total time difference of particle transport between systems with different interface steepness is dominated by the transports from one heat source to another heat source. The cumulative distribution curve of the total time is plotted in Fig. 6(d). It can be found that the total time of particle transport in the forward direction in asymmetric homojunctions increases with the increasing interface steepness. Similarly, one can find that the total time of particle transport in the backward direction decreases with the increasing interface steepness. Consequently, the forward heat flow decreases while the backward heat flow increases when the interface steepness of the asymmetric homojunction increases.

- [1] N. Li, J. Ren, L. Wang, G. Zhang, P. Hanggi, and B. Li, *Rev. Mod. Phys.* **84**, 1045 (2012).
- [2] N. Yang, X. Xu, G. Zhang, and B. Li, *AIP Adv.* **2**, 041410 (2012).
- [3] B. Li, L. Wang, and G. Casati, *Phys. Rev. Lett.* **93**, 184301 (2004).
- [4] D. Segal and A. Nitzan, *Phys. Rev. Lett.* **94**, 034301 (2005).
- [5] C. Chang, D. Okawa, A. Majumdar, and A. Zettl, *Science* **314**, 1121 (2006).
- [6] L. A. Wu and D. Segal, *Phys. Rev. Lett.* **102**, 095503 (2009).
- [7] T. Ruokola, T. Ojanen, and A. P. Jauho, *Phys. Rev. B* **79**, 144306 (2009).
- [8] H. Wang, S. Hu, K. Takahashi, X. Zhang, H. Takamatsu, and J. Chen, *Nat. Commun.* **8**, 15843 (2017).
- [9] R. Shrestha, Y. Luan, X. Luo, S. Shin, T. Zhang, P. Smith, W. Gong, M. Bockstaller, T. Luo, R. Chen, K. Hippalgaonkar, and S. Shen, *Nat. Commun.* **11**, 4346 (2020).
- [10] Y. Yang, H. Chen, H. Wang, N. Li, and L. Zhang, *Phys. Rev. E* **98**, 042131 (2018).
- [11] B. Li, L. Wang, and G. Casati, *Appl. Phys. Lett.* **88**, 143501 (2006).
- [12] D. He, S. Buyukdagli, and B. Hu, *Phys. Rev. B* **80**, 104302 (2009).
- [13] K. Joulain, J. Drevillon, Y. Ezzahri, and J. Ordonez-Miranda, *Phys. Rev. Lett.* **116**, 200601 (2016).
- [14] A. Fornieri, G. Timossi, R. Bosisio, P. Solinas, and F. Giazotto, *Phys. Rev. B* **93**, 134508 (2016).
- [15] Y. Yang, D. Ma, Y. Zhao, and L. Zhang, *J. Appl. Phys.* **127**, 195301 (2020).
- [16] Q. Ruan and L. Wang, *Phys. Rev. Research* **2**, 023087 (2020).
- [17] Y. Yang, X. Li, and L. Zhang, *Chin. Phys. Lett.* **38**, 016601 (2021).
- [18] L. Wang and B. Li, *Phys. Rev. Lett.* **101**, 267203 (2008).
- [19] C. Guarcello, P. Solinas, A. Braggio, M. Di Ventra, and F. Giazotto, *Phys. Rev. Appl.* **9**, 014021 (2018).
- [20] A. M. Morsya, R. Biswas, and M. L. Povinelli, *APL Photonics* **4**, 010804 (2019).
- [21] L. Wang and B. Li, *Phys. Rev. Lett.* **99**, 177208 (2007).
- [22] F. Paolucci, G. Marchegiani, E. Strambini, and F. Giazotto, *Phys. Rev. Appl.* **10**, 024003 (2018).
- [23] C. Kathmann, M. Reina, R. Messina, P. Ben-Abdallah, and S.-A. Biehs, *Sci. Rep.* **10**, 3596 (2020).
- [24] N. Yang, G. Zhang, and B. Li, *Appl. Phys. Lett.* **95**, 033107 (2009).
- [25] L. Zhang, J.-S. Wang, and B. Li, *Phys. Rev. B* **81**, 100301(R) (2010).
- [26] H. A. Lorentz, *Proc. K. Ned. Akad. Wet.* **7**, 438 (1905).
- [27] D. Alonso, R. Artuso, G. Casati, and I. Guarneri, *Phys. Rev. Lett.* **82**, 1859 (1999).
- [28] H. Larralde, F. Leyvraz, and C. Mejia-Monasterio, *J. Stat. Phys.* **113**, 197 (2003).
- [29] G. Casati, C. Mejia-Monasterio, and T. Prosen, *Phys. Rev. Lett.* **98**, 104302 (2007).
- [30] H. Chen, H. Wang, Y. Yang, N. Li, and L. Zhang, *Phys. Rev. E* **98**, 032131 (2018).
- [31] H. Chen, Y. Yang, Z. Yu, M. Zhong, and L. Zhang, *Phys. Rev. E* **101**, 042129 (2020).
- [32] B. Moran, W. G. Hoover, and S. Bestiale, *J. Stat. Phys.* **48**, 709 (1987).
- [33] H. Wang, Y. Yang, H. Chen, N. Li, and L. Zhang, *Phys. Rev. E* **99**, 062111 (2019).
- [34] R. Dickman and R. Motai, *Phys. Rev. E* **89**, 032134 (2014).